Departing from Thermality of Analogue Hawking Radiation in a Bose-Einstein Condensate

M. Isoard and N. Pavloff
Université Paris-Saclay, CNRS, LPTMS, 91405 Orsay

(Received 5 September 2019; accepted 9 January 2020; published 10 February 2020)

We study the quantum fluctuations in a one-dimensional Bose-Einstein condensate realizing an analogous acoustic black hole. The taking into account of evanescent channels and of zero modes makes it possible to accurately reproduce recent experimental measurements of the density correlation function. We discuss the determination of Hawking temperature and show that in our model the analogous radiation presents some significant departure from thermality.

DOI: 10.1103/PhysRevLett.124.060401

The Hawking effect [1] being of kinematic origin [2] can be transposed to analogue systems, as first proposed by Unruh [3]. Among the various platforms that have been proposed for observing induced or spontaneous analogous Hawking radiation and related phenomena, the ones for which the experimental activity is currently the most intense are surface water waves [4–10], nonlinear light [11–17], excitonic polaritons [18], and Bose-Einstein condensed atomic vapors [19–22].

Because of their low temperature, their intrinsic quantum nature, and the high experimental control achieved in these systems, Bose-Einstein condensates (BECs) seem particularly suitable for studying analogue Hawking effect. Steinhauer and colleagues have undertaken several studies of quasiunidimensional configurations, making it possible to realize analogue black hole horizons in BEC systems, and made claims of observation of Hawking radiation [20–22]. Their results have triggered the interest of the community [23–33] and generated a vivid debate [34,35]. One of the goals of the present Letter is to contribute to this debate, and to partially close it, at least in what concerns density correlations around an analogue black hole horizon. A definite theoretical answer can be obtained thanks to a remark that had been overlooked in previous works: one needs to develop the quasiparticle operator on a complete basis set for properly describing the density fluctuations. This is achieved in the first part of this Letter, and we apply this theoretical approach to the analysis of the experimental results of Ref. [22].

While in general relativity the thermality of the Hawking radiation is constrained by the laws of black hole thermodynamics, no such general principle is expected to hold for analogue systems [2]. It is nonetheless commonly accepted that the spectrum of analogous Hawking radiation only weakly departs from thermality [36–38], and that all relevant features of an analogue system can be understood on the basis of a hydrodynamical, long wavelength description. However, the phenomenology of analogous systems provides mechanisms supporting the impossibility of a perfectly thermal analogue Hawking radiation [39]. In the second part of this Letter we argue that in the BEC case we are considering, it is legitimate to determine a Hawking temperature from the information encoded in the density correlation function, but we show that some features of the radiative process at hand significantly depart from thermality and propose a procedure for confirming our view.

We consider a one-dimensional configuration in which the quantum field $\hat{\Psi}(x,t)$ is a solution of the Gross-Pitaevskii equation

$$i\hbar\partial_t\hat{\Psi} = -\frac{\hbar^2}{2m}\partial_x^2\hat{\Psi} + [g\hat{n} + U(x)]\hat{\Psi}. \tag{1}$$

In this equation m is the mass of the atoms, $\hat{n} = \hat{\Psi}^\dagger\hat{\Psi}$, and the term $g\hat{n}$ describes the effective repulsive atomic interaction ($g > 0$). We have studied several external potentials $U(x)$ making it possible to engineer a sonic horizon, but we only present here the results for a step function: $U(x) = -U_0\Theta(x)$ with $U_0 > 0$. The reason for this choice is twofold: (i) This potential has been realized experimentally in Refs. [21,22]; (ii) from the three configurations analyzed in Ref. [31], this is the one that leads to the signal of quantum nonseparability which is the largest and the most resilient to temperature effects.

In the spirit of Bogoliubov's approach, we write the quantum field as

$$\hat{\Psi}(x,t) = \exp(-i\mu t/\hbar)[\Phi(x) + \hat{\psi}(x,t)], \tag{2}$$

where μ is the chemical potential. $\Phi(x)$ is a classical field describing the stationary condensate and $\hat{\psi}(x,t)$ accounts for small quantum fluctuations. Although such a separation is not strictly valid in one dimension, it has been argued in Ref. [31] that it constitutes a valid approximation over a large range of one-dimensional densities. In the case we

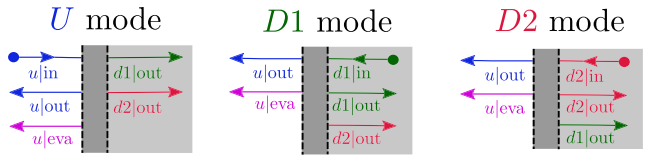

FIG. 1. Sketch of the different channels contributing to the incoming quantum modes U, $D1$, and $D2$. In each plot the background BEC propagates from left to right, the white region corresponds to the upstream subsonic flow, the gray one to the interior of the analogous black hole (downstream supersonic flow), and the region of the horizon is represented by the dark gray shaded interface. The Hawking channel and its partner are labeled $u|$out and $d2|$out. The $d1|$out channel is a companion propagating away from the horizon, inside the analogous black hole region. Each mode (U, $D1$, and $D2$) is seeded by an ingoing channel ($u|$in, $d1|$in, and $d2|$in) whose group velocity is directed towards the horizon.

consider, Φ is a solution of the classical Gross-Pitaevskii equation describing a sonic horizon: the $x<0$ profile is half a dark soliton [40], with $\Phi(x\to-\infty)=\sqrt{n_u}\exp(ik_u x)$, where n_u and $V_u=mk_u/\hbar$ (>0) are the upstream asymptotic density and velocity, respectively. The downstream ($x>0$) flow of the condensate corresponds to a plane wave: $\Phi(x>0)=\sqrt{n_d}\exp(ik_d x-i\pi/2)$. The asymptotic upstream and downstream sound velocities are $c_{(u,d)}=\sqrt{gn_{(u,d)}/m}$. The analogous black hole configuration corresponds to a flow that is asymptotically upstream subsonic ($V_u<c_u$) and downstream supersonic ($\hbar k_d/m=V_d>c_d$).

We describe the quantum fluctuations on top of this classical field within a linearized approach. The relevant modes are identified by using the asymptotic ingoing (i.e., directed towards the acoustic horizon) and outgoing channels, far from the horizon. As discussed in previous references [41–45] and recalled in [46], the Bogoliubov dispersion relation supports a decomposition of $\hat{\psi}$ onto three incoming modes that we denote as U, $D1$, and $D2$. For instance, the U mode is seeded by an upstream incoming wave that we denote as $u|$in, which propagates towards the horizon with a long wavelength group velocity V_u+c_u. It is scattered onto two outgoing transmitted channels (propagating in the analogue black hole away from the horizon), which we denote as $d1|$out and $d2|$out with respective long wavelength group velocities V_d+c_d and V_d-c_d (both positive) and one outgoing reflected channel (propagating away from the horizon, outside of the analogue black hole, with long wavelength group velocity $V_u-c_u<0$). The corresponding three scattering coefficients are denoted as $S_{d1,u}$, $S_{d2,u}$, and $S_{u,u}$. There is also an upstream evanescent wave ($u|$eva) that carries no current, does not contribute to the S matrix, but is important for fulfilling the continuity relations at $x=0$. The situation is schematically depicted in Fig. 1.

The frequency-dependent boson operators associated to the three incoming modes U, $D1$, and $D2$ are denoted as $\hat{b}_U$, $\hat{b}_{D1}$, and $\hat{b}_{D2}$; they obey the commutation relations $[\hat{b}_L(\omega),\hat{b}^\dagger_{L'}(\omega')]=\delta_{L,L'}\delta(\omega-\omega')$. In addition, Bose-Einstein condensation is associated with a spontaneously broken $U(1)$ symmetry that implies the existence of supplementary zero modes of the linearized version of (1). As discussed in Ref. [50], one is lead to introduce two new operators $\hat{\mathcal{P}}$ and $\hat{\mathcal{Q}}$ accounting for the global phase degree of freedom, and the correct expansion of the quantum fluctuation field reads

$$\begin{aligned}\hat{\psi}(x,t)=&-i\Phi(x)\hat{\mathcal{Q}}+iq(x)\hat{\mathcal{P}}+\int_0^\infty\frac{d\omega}{\sqrt{2\pi}}\sum_{L\in\{U,D1\}}\\&\times[u_L(x,\omega)e^{-i\omega t}\hat{b}_L(\omega)+v_L^*(x,\omega)e^{i\omega t}\hat{b}_L^\dagger(\omega)]\\&+\int_0^\Omega\frac{d\omega}{\sqrt{2\pi}}[u_{D2}(x,\omega)e^{-i\omega t}\hat{b}^\dagger_{D2}(\omega)\\&+v^*_{D2}(x,\omega)e^{i\omega t}\hat{b}_{D2}(\omega)].\end{aligned}\tag{3}$$

In this expression the u_L's and v_L's are the usual Bogoliubov coefficients (their explicit form is given for instance in Ref. [44]), and the quantization of the $D2$ mode is atypical, as discussed in several previous references [41,42,51]. The function $q(x)$ is one of the components of the zero eigenmodes; see [46]. Omitting the contribution of the zero mode operators $\hat{\mathcal{P}}$ and $\hat{\mathcal{Q}}$ would correspond to using an incomplete basis set for the expansion of the quantum fluctuations; in other words, their contribution is essential for verifying the correct commutation relation $[\hat{\psi}(x,t),\hat{\psi}^\dagger(y,t)]=\delta(x-y)$. The operator $\hat{\mathcal{Q}}$ is associated with the global phase of the condensate. $\hat{\mathcal{P}}$ is the canonical conjugate operator ($[\hat{\mathcal{Q}},\hat{\mathcal{P}}]=i$) that typically appears in the quadratic Hamiltonian $\hat{H}_{\rm quad}$ describing the dynamics of the quantum fluctuations with a $\hat{\mathcal{P}}^2$ contribution, while $\hat{\mathcal{Q}}$ does not [50,52,53]. This means that the degree of liberty associated with the broken symmetry has no restoring force—as expected on physical grounds—and that the zero excitation quantum state $|\mathrm{BH}\rangle$ describing the analogous black hole configuration verifies $\hat{\mathcal{P}}|\mathrm{BH}\rangle=0$ and $\hat{b}_L(\omega)|\mathrm{BH}\rangle=0$ for $L\in\{U,D1,D2\}$.

Once the appropriate expansion (3) has been performed, and the correct quantum state $|\mathrm{BH}\rangle$ has been identified, one can compute the density correlation function,

$$\begin{aligned}G_2(x,y)=&\langle{:}\hat{n}(x,t)\hat{n}(y,t){:}\rangle-\langle\hat{n}(x,t)\rangle\langle\hat{n}(y,t)\rangle\\\simeq&\,\Phi(x)\Phi^*(y)\langle\hat{\psi}^\dagger(x,t)\hat{\psi}(y,t)\rangle\\&+\Phi(x)\Phi(y)\langle\hat{\psi}^\dagger(x,t)\hat{\psi}^\dagger(y,t)\rangle+\text{c.c.}\end{aligned}\tag{4}$$

In this equation, the symbol : denotes normal ordering and the final expression is the Bogoliubov evaluation of G_2, encompassing the effects of quantum fluctuations at leading order. At zero temperature, the average $\langle\cdots\rangle$ in Eq. (4) is taken over the state $|\mathrm{BH}\rangle$. Although this state is thermodynamically unstable and cannot support a thermal

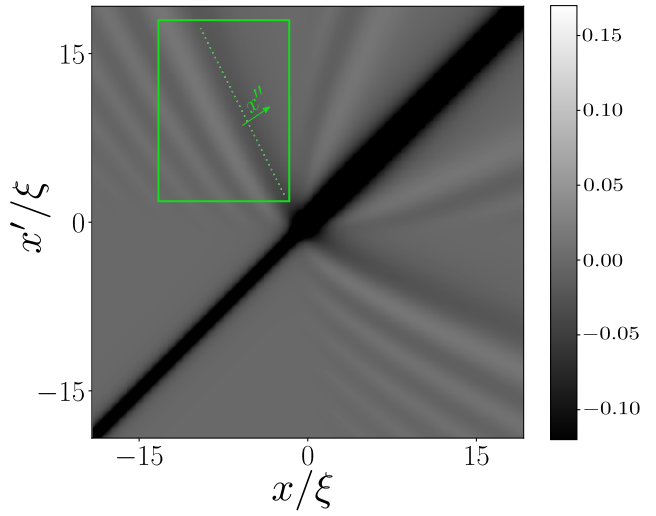

FIG. 2. Intensity plot of the dimensionless correlation function $\xi(n_u n_d)^{-1/2} G_2(x, x')$ for x and x' close to the horizon. The parameter $\xi = \sqrt{\xi_u \xi_d}$ is the geometrical mean of the healing lengths ξ_u and ξ_d, where $\xi_{(u/d)} = \hbar(m g n_{(u,d)})^{-1/2}$. The line of anticorrelation in the upper left and lower right quadrants corresponds to the merging close to the horizon of the Hawking-partner $(u|\text{out} - d2|\text{out})$ and Hawking-companion $(u|\text{out} - d1|\text{out})$ correlations. The green rectangle delimits the region where we average G_2 for comparison with experimental data (see Fig. 3).

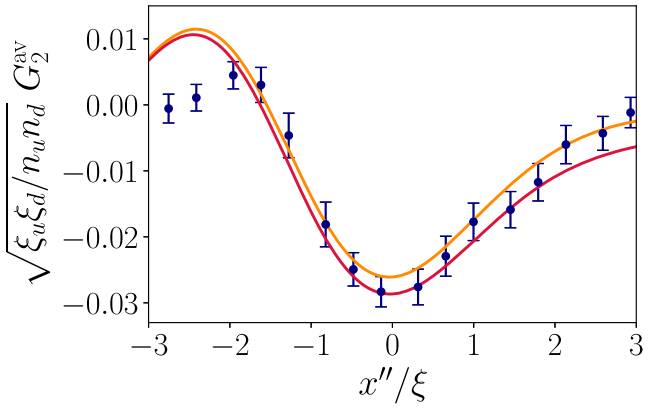

FIG. 3. Red solid line: zero temperature density correlation function $G_2^{\text{av}}(x, x')$ plotted as a function of x''. The blue dots with error bars are the results of Ref. [22]. The orange solid line is the finite temperature result for $k_B T = 0.2 g n_u$, i.e., $T \simeq 1.9 T_H$.

distribution, finite temperature effects can still be included as explained for instance in Refs. [31,41,42].

In 2008 a collaboration between teams from Bologna and Trento [54,55] pointed out that, in the presence of a horizon, G_2 should exhibit nonlocal features resulting from correlations between the different outgoing channels, in particular, between the Hawking quantum and its partner ($u|\text{out} - d2|\text{out}$ correlation in our terminology). The importance of this remark lies in the fact that, due to the weak Hawking temperature T_H (at best one fourth of the chemical potential [44]), the direct Hawking radiation is expected to be hidden by thermal fluctuations, whereas density correlations should survive temperature effects in typical settings [42]. This idea has been used to analyze the Hawking signal in Ref. [22], where a stationary correlation pattern was measured in the vicinity of the horizon. In this region, it is important for a theoretical treatment to account for the position dependence of the background density and to include the contribution of the evanescent channels in the expansion (3). We also checked that it is essential to take into account the contribution of the zero modes to obtain a sensible global description of the quantum fluctuations. The corresponding two-dimensional plot of the density correlation pattern is represented in Fig. 2. G_2 has been computed at zero temperature, for $V_d/c_d = 2.90$, which imposes $V_u/c_u = 0.59$ [44,46]. This value is chosen to reproduce the experimental configuration studied in Ref. [22]. The dotted line in the upper left quadrant of Fig. 2 marks the anticorrelation curve that results from the Hawking-partner $(u|\text{out} - d2|\text{out})$ and Hawking-companion $(u|\text{out} - d1|\text{out})$ correlations. We find that these two correlation lines, which separate at large distance from the horizon [42,44,55], merge close to the horizon, as also observed experimentally.

A precise comparison of our results with experiment can be achieved by following the procedure used in Ref. [22], which consists in averaging G_2 over the region inside the green rectangle represented in Fig. 2. One defines a local coordinate x'' that is orthogonal to the locus of the minima of G_2, and one plots the averaged G_2 (denoted as G_2^{av}) as a function of the variable x''. This is done in Fig. 3. We insist that the good agreement between our approach and the experimental results can only be achieved through a correct description of the quantum fluctuations—Eq. (3)—including the contribution of zero modes and evanescent channels.

It has been noticed by Steinhauer [56] that the determination of $G_2(x, x')$ in the upper left (or lower right) quadrant of the (x, x') plane makes it possible to evaluate the Hawking temperature thanks to the relation

$$S_{u,d2}(\omega) S^*_{d2,d2}(\omega) = \langle \hat{c}_U(\omega) \hat{c}_{D2}(\omega) \rangle = \frac{\mathcal{S}_0^{-1}}{\sqrt{n_u n_d L_u L_d}} \int_{-L_u}^{0} dx \int_{0}^{L_d} dx' e^{-i(k_H x + k_P x')} G_2(x, x'). \tag{5}$$

In this expression S is the matrix that describes the scattering of the different channels onto each other, and $\mathcal{S}_0(\omega) = (u_{k_H} + v_{k_H})(u_{k_P} + v_{k_P})$ is the static structure factor, where the u_k's and the v_k's are the standard Bogoliubov amplitudes of excitations of momentum k (see, e.g., Refs. [57,58]). The $\hat{c}_L$'s are outgoing modes related to the incoming ones by the S matrix [42]

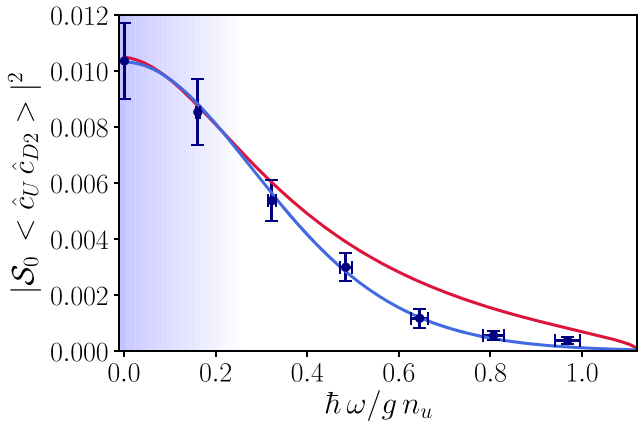

FIG. 4. Hawking-partner correlation signal represented as a function of the dimensionless energy. The red solid curve is the theoretical result from Eq. (5). The dots with error bars are from Ref. [22]. They are obtained after processing the experimental result for G_2 by means of the Fourier transform (5). The blue region corresponds to a domain where the ratio of Hawking and partner wave vectors is equal to its long wavelength value within a 10% accuracy. The blue solid curve is the theoretical result obtained by neglecting dispersive effects in Eq. (5) and discarding the contribution of the companion $d1|$out channel (see the text).

$$\begin{pmatrix} \hat{c}_U \\ \hat{c}_{D1} \\ \hat{c}^\dagger_{D2} \end{pmatrix} = \begin{pmatrix} S_{u,u} & S_{u,d1} & S_{u,d2} \\ S_{d1,u} & S_{d1,d1} & S_{d1,d2} \\ S_{d2,u} & S_{d2,d1} & S_{d2,d2} \end{pmatrix} \begin{pmatrix} \hat{b}_U \\ \hat{b}_{D1} \\ \hat{b}^\dagger_{D2} \end{pmatrix}. \quad (6)$$

The Fourier transform of G_2 in Eq. (5) is performed at fixed ω, for wave vectors $k_H(\omega)$ and $k_P(\omega)$, which are the momenta relative to the condensate of a Hawking quantum and its partner ($u|$out and $d2|$out channels in our terminology) having an energy $\hbar\omega$ in the laboratory frame. The integration region $[-L_u, 0] \times [0, L_d]$ lies in the upper left quadrant of Fig. 2, and should be adapted for each value of ω in such a way that [31,59]

$$\frac{L_u}{|V_{g,H}(\omega)|} = \frac{L_d}{V_{g,P}(\omega)}, \quad (7)$$

where $V_{g,H}(\omega)$ [$V_{g,P}(\omega)$] is the group velocity of a Hawking quantum (of a partner) of energy $\hbar\omega$. We have checked that once the prescription (7) is fulfilled, formula (5) is very well verified [46]. It is then intriguing to observe that, while theory and experiment both agree on the value of G_2 in real space (Fig. 3), they do not for the correlation $\langle \hat{c}_U(\omega)\hat{c}_{D2}(\omega)\rangle$: as can bee seen in Fig. 4, the agreement is restricted to the low energy regime. This is the bluish region in the figure, which corresponds to a domain where the ratio $k_H(\omega)/k_P(\omega)$ is equal to its long wavelength value $(c_u - V_u)/(c_d - V_d)$ with an error less that 10%.

Let us discuss this discrepancy in some detail. The interest of Eq. (5) lies in the fact that the scattering matrix coefficient $S_{u,d2}$ is the equivalent of the Hawking β parameter: its squared modulus is expected to behave as a Bose thermal distribution $n_{T_H}(\omega)$ with an effective temperature T_H, the Hawking temperature [1]. In an analogous system such as ours, because of dispersive effects, this equivalence is only valid in the long wavelength limit, typically in the blue region of Fig. 4. This suggests a possible manner to reconcile theory and experiment: we assume that the ratio $k_H(\omega)/k_P(\omega)$ is ω independent and equal to its low energy value, $(c_u - V_u)/(c_d - V_d)$ (this value is denoted as $\tan\theta$ in Refs. [21,22]). We also assume that, in the scattering process schematically illustrated in Fig. 1 for the $D2$ mode, the companion $d1|$out channel plays a negligible role, so that the $|S_{d1,d2}|^2$ term can be omitted in the normalization condition $|S_{d2,d2}|^2 = 1 + |S_{u,d2}|^2 + |S_{d1,d2}|^2$ of the S matrix (see, e.g., Ref. [42]). Then one obtains

$$|S_{u,d2}|^2 |S_{d2,d2}|^2 \simeq n_{T_H}(\omega)[1 + n_{T_H}(\omega)]. \quad (8)$$

Using the experimental values from Ref. [22] for V_α and c_α ($\alpha \in \{u, d\}$) and for the Hawking temperature T_H leads, within approximation (8), to the blue curve of Fig. 4 that agrees with the results published in Ref. [22] (blue dots with error bars). It is important to note that this procedure is self-consistent in the following sense: If one performs numerically the Fourier transform (5) over a domain that, instead of fulfilling the relation (7), verifies the ω-independent condition $L_u/|V_u - c_u| = L_d/(V_d - c_d)$, appropriate in a nondispersive, long wavelength approximation, one obtains a result (not shown for legibility, but see [46]) close to a thermal spectrum, i.e., to the blue curve in Fig. 4. Although this procedure is self-consistent, it is not fully correct, as can be checked by the fact that the resulting value of $\langle \hat{c}_U(\omega)\hat{c}_{D2}(\omega)\rangle$ only agrees with the exact one (red curve in Fig. 4) in the long wavelength limit. Stated differently: this procedure leads to the erroneous conclusion that the radiation is fully thermal. However, since all approaches coincide in the long wavelength regime (blue colored region of Fig. 4), they all lead to the correct determination of the Hawking temperature. For a flow with $V_d/c_d = 2.9$, our theoretical treatment yields $k_B T_H/(g n_u) = 0.106$, whereas the experimental value reported for this quantity in Ref. [22] is 0.124 (corresponding to a Hawking temperature $T_H = 0.35$ nK).

In conclusion, our work sheds a new light on the study of quantum correlations around an analogous black hole horizon, and on the corresponding Hawking temperature. From a theoretical point of view, we argue that the contribution of zero modes is essential for constructing a complete basis set necessary to obtain an accurate description of the quantum fluctuations. This claim is supported by the excellent agreement we obtain when comparing our results with recent experimental ones. On the experimental side, we substantiate the determination of the Hawking

temperature presented in Ref. [22], although we find that the Hawking spectrum is not thermal for all wavelengths. We identify a natural but unfounded procedure for analyzing the information encoded in $G_2(x,x')$ that leads to the opposite conclusion; we show that, within our approach, an alternative analysis of the correlation pattern accurately accounts for nonhydrodynamical effects. It would thus be interesting to reanalyze the data published in Ref. [22] to investigate if the windowing (7) we propose for Eq. (5) modifies the experimental conclusion for the Hawking-partner correlation signal and confirms the departure from thermality we predict.

We acknowledge fruitful discussions with I. Carusotto, M. Lewenstein, and J. Steinhauer, whom we also thank for providing us with experimental data.

[1] S. W. Hawking, Nature (London) **248**, 30 (1974); Commun. Math. Phys. **43**, 199 (1975).
[2] M. Visser, Phys. Rev. Lett. **80**, 3436 (1998).
[3] W. G. Unruh, Phys. Rev. Lett. **46**, 1351 (1981).
[4] G. Rousseaux, C. Mathis, P. Maïssa, T. G. Philbin, and U. Leonhardt, New J. Phys. **10**, 053015 (2008).
[5] S. Weinfurtner, E. W. Tedford, M. C. J. Penrice, W. G. Unruh, and G. A. Lawrence, Phys. Rev. Lett. **106**, 021302 (2011).
[6] L.-P. Euvé, F. Michel, R. Parentani, T. G. Philbin, and G. Rousseaux, Phys. Rev. Lett. **117**, 121301 (2016).
[7] V. Cardoso, A. Coutant, M. Richartz, and S. Weinfurtner, Phys. Rev. Lett. **117**, 271101 (2016).
[8] T. Torres, S. Patrick, A. Coutant, M. Richartz, E. W. Tedford, and S. Weinfurtner, Nat. Phys. **13**, 833 (2017).
[9] L.-P. Euvé, S. Robertson, N. James, A. Fabbri, and G. Rousseaux, arXiv:1806.05539.
[10] H. Goodhew, S. Patrick, C. Gooding, and S. Weinfurtner, arXiv:1905.03045.
[11] T. G. Philbin, C. Kuklewicz, S. Robertson, S. Hill, F. König, and U. Leonhardt, Science **319**, 1367 (2008).
[12] F. Belgiorno, S. L. Cacciatori, M. Clerici, V. Gorini, G. Ortenzi, L. Rizzi, E. Rubino, V. G. Sala, and D. Faccio, Phys. Rev. Lett. **105**, 203901 (2010).
[13] E. Rubino, F. Belgiorno, S. L. Cacciatori, M. Clerici, V. Gorini, G. Ortenzi, L. Rizzi, V. G. Sala, M. Kolesik, and D. Faccio, New J. Phys. **13**, 085005 (2011).
[14] M. Elazar, V. Fleurov, and S. Bar-Ad, Phys. Rev. A **86**, 063821 (2012).
[15] K. E. Webb, M. Erkintalo, Y. Xu, N. G. R. Broderick, J. M. Dudley, G. Genty, and S. G. Murdoch, Nat. Commun. **5**, 4969 (2014).
[16] D. Vocke, C. Maitland, A. Prain, K. E. Wilson, F. Biancalana, E. M. Wright, F. Marino, and D. Faccio, Optica **5**, 1099 (2018).
[17] J. Drori, Y. Rosenberg, D. Bermudez, Y. Silberberg, and U. Leonhardt, Phys. Rev. Lett. **122**, 010404 (2019).
[18] H. S. Nguyen, D. Gerace, I. Carusotto, D. Sanvitto, E. Galopin, A. Lemaître, I. Sagnes, J. Bloch, and A. Amo, Phys. Rev. Lett. **114**, 036402 (2015).
[19] O. Lahav, A. Itah, A. Blumkin, C. Gordon, S. Rinott, A. Zayats, and J. Steinhauer, Phys. Rev. Lett. **105**, 240401 (2010).
[20] J. Steinhauer, Nat. Phys. **10**, 864 (2014).
[21] J. Steinhauer, Nat. Phys. **12**, 959 (2016).
[22] J. R. M. de Nova, K. Golubkov, V. I. Kolobov, and J. Steinhauer, Nature (London) **569**, 688 (2019).
[23] F. Michel and R. Parentani, Phys. Rev. A **91**, 053603 (2015).
[24] F. Michel, J.-F. Coupechoux, and R. Parentani, Phys. Rev. D **94**, 084027 (2016).
[25] M. Tettamanti, S. L. Cacciatori, A. Parola, and I. Carusotto, Europhys. Lett. **114**, 60011 (2016).
[26] J. R. M. de Nova, S. Finazzi, and I. Carusotto, Phys. Rev. A **94**, 043616 (2016).
[27] A. Finke, P. Jain, and S. Weinfurtner, New J. Phys. **18**, 113017 (2016).
[28] Y.-H. Wang, T. Jacobson, M. Edwards, and C. W. Clark, SciPost Phys. **3**, 022 (2017).
[29] A. Parola, M. Tettamanti, and S. L. Cacciator, Europhys. Lett. **119**, 50002 (2017).
[30] S. Robertson, F. Michel, and R. Parentani, Phys. Rev. D **96**, 045012 (2017).
[31] A. Fabbri and N. Pavloff, SciPost Phys. **4**, 019 (2018).
[32] A. Coutant and S. Weinfurtner, Phys. Rev. D **97**, 025006 (2018).
[33] J. M. Gomez Llorente and J. Plata, J. Phys. B **52**, 075004 (2019).
[34] U. Leonhardt, Ann. Phys. (Berlin) **530**, 1700114 (2018).
[35] J. Steinhauer, Ann. Phys. (Berlin) **530**, 1700459 (2018).
[36] W. G. Unruh, Phys. Rev. D **51**, 2827 (1995).
[37] S. Corley and T. Jacobson, Phys. Rev. D **54**, 1568 (1996).
[38] S. Corley, Phys. Rev. D **55**, 6155 (1997).
[39] T. Jacobson, Phys. Rev. D **44**, 1731 (1991).
[40] P. Leboeuf, N. Pavloff, and S. Sinha, Phys. Rev. A **68**, 063608 (2003).
[41] J. Macher and R. Parentani, Phys. Rev. A **80**, 043601 (2009).
[42] A. Recati, N. Pavloff, and I. Carusotto, Phys. Rev. A **80**, 043603 (2009).
[43] A. Coutant, R. Parentani, and S. Finazzi, Phys. Rev. D **85**, 024021 (2012).
[44] P.-É. Larré, A. Recati, I. Carusotto, and N. Pavloff, Phys. Rev. A **85**, 013621 (2012).
[45] D. Boiron, A. Fabbri, P.-É. Larré, N. Pavloff, C. I. Westbrook, and P. Ziń, Phys. Rev. Lett. **115**, 025301 (2015).
[46] See Supplemental Material at http://link.aps.org/supplemental/10.1103/PhysRevLett.124.060401 which recalls previous results, details some characteristics of the zero modes and of the analysis of the Hawking spectrum and includes Refs. [47–49].
[47] P. Villain, M. Lewenstein, R. Dum, Y. Castin, L. You, A. Imamoğlu, and T. A. B. Kennedy, J. Mod. Opt. **44**, 1775 (1997).
[48] N. Bilas and N. Pavloff, Phys. Rev. A **72**, 033618 (2005).
[49] P. Deuar, A. G. Sykes, D. M. Gangardt, M. J. Davis, P. D. Drummond, and K. V. Kheruntsyan, Phys. Rev. A **79**, 043619 (2009).
[50] M. Lewenstein and L. You, Phys. Rev. Lett. **77**, 3489 (1996).
[51] U. Leonhardt, T. Kiss, and P. Öhberg, J. Opt. B **5**, S42 (2003).

[52] P. Ring and P. Shuck, *The Nuclear Many-Body Problem* (Springer-Verlag, Berlin, 1980).
[53] J. P. Blaizot and G. Ripka, *Quantum Theory of Finite Systems* (MIT Press, Cambridge, MA, 1986).
[54] R. Balbinot, A. Fabbri, S. Fagnocchi, A. Recati, and I. Carusotto, Phys. Rev. A **78**, 021603(R) (2008).
[55] I. Carusotto, S. Fagnocchi, A. Recati, R. Balbinot, and A. Fabbri, New J. Phys. **10**, 103001 (2008).
[56] J. Steinhauer, Phys. Rev. D **92**, 024043 (2015).
[57] C. J. Pethick and H. Smith, *Bose-Einstein Condensation in Dilute Gases* (Cambridge University Press, Cambridge, England, 2002).
[58] L. P. Pitaevskii and S. Stringari, *Bose-Einstein Condensation*, International Series of Monographs on Physics (Oxford University Press, Oxford, United Kingdom, 2016).
[59] J. R. M. de Nova, F. Sols, and I. Zapata, New J. Phys. **17**, 105003 (2015).

Supplemental material to: Departing from thermality of analogue Hawking radiation in a Bose-Einstein condensate

M. Isoard[1] and N. Pavloff[1]

[1] *Université Paris-Saclay, CNRS, LPTMS, 91405 Orsay, France*

THE BACKGROUND FLOW AND DENSITY PROFILES

We recall here the properties of the background transonic flow $\Phi(x)$ realizing an analogue black hole horizon [1]. $\Phi(x)$ is solution of the classical stationary Gross-Pitaevskii equation

$$\mu\Phi = -\frac{\hbar^2}{2m}\partial_x^2\Phi + [g\,n(x) + U(x)]\,\Phi\ , \tag{S1}$$

with $n(x) = |\Phi(x)|^2$ and $U(x) = -U_0\Theta(x)$, where Θ is the Heaviside step function and $U_0 > 0$. There exists a stationary solution of this equation which is half a dark soliton glued at $x = 0$ to a plane wave [2]:

$$\Phi(x) = \begin{cases} \sqrt{n_u}\,\exp(ik_u x)\,\chi_u(x) \equiv \Phi_u(x) & \text{for } x \le 0, \\ \sqrt{n_d}\,\exp(ik_d x - i\pi/2) \equiv \Phi_d(x) & \text{for } x \ge 0. \end{cases} \tag{S2}$$

where

$$\chi_u(x) = \cos\theta\,\tanh(x\cos\theta/\xi_u) - i\sin\theta. \tag{S3}$$

In these equations n_u and n_d are the asymptotic upstream and downstream densities, $\xi_u = \hbar(mgn_u)^{-1/2}$ is the upstream healing length and $\sin\theta = V_u/c_u$ where V_u and $c_u = \hbar/(m\xi_u)$ are the asymptotic flow and sound velocities. The downstream flow and sound velocity are $V_d = \hbar k_d/m$ and $c_d = \sqrt{gn_d/m}$. The chemical potential μ in Eq. (S1) verifies

$$\mu = \tfrac{1}{2}mV_u^2 + gn_u = \tfrac{1}{2}mV_d^2 + gn_d - U_0. \tag{S4}$$

The matching conditions at $x = 0$ impose

$$\frac{V_d}{V_u} = \frac{n_u}{n_d} = \left(\frac{c_u}{V_u}\right)^2 = \frac{V_d}{c_d}. \tag{S5}$$

Hence, in this configuration, which we denote as "waterfall", the upstream and downstream Mach numbers (V_u/c_u and V_d/c_d) are not independent. We chose to take the same downstream Mach number than in the experiment [3]: $V_d/c_d = 2.9$. From (S5) this imposes $V_u/c_u = 0.59$, different from the experimental value ($V_u/c_u|_{\rm exp} = 0.44$). This difference indicates that the experiment is not exactly in a waterfall configuration. This is probably due to the fact that the experimental external potential is not exactly a Heaviside function. It could also be that the experimental flow has not yet reached a fully stationary state. This difference does not preclude a very good agreement with the experimental density correlation pattern (as observed in Fig. 3 of the main text); however, it explains why we cannot reproduce with the same accuracy the behavior of the density correlation function $G_2(x, x')$ in all the quadrants of Fig. 2 of the main text: the $d1|\text{out} - d2|\text{out}$ correlation line (upper right quadrant of Fig. 2 of the main text) does not exactly superimposes with the experimental one. We take the same value of V_d/c_d as in the experiment, because this is the choice which gives the better account of experiment in the upper left quadrant of Fig. 2 of the main text, which is the core of the discussion of Ref. [3].

THE BOGOLIUBOV-DE GENNES EQUATIONS

In this section we present the construction of expansion (3) of the main text. The first part of the section is devoted to the definition of the usual Bogoliubov modes, and is an abridged version of a discussion which can be found in Ref. [1]; the second part concerns the construction of the zero modes and comprises a general discussion (from Refs. [4–6]) followed by the explicit form of these modes in the situation we consider [Eqs. (S14) and (S15)].

The simplest way to set up an eigen-basis set for expanding the quantum fluctuation operator is to treat $\hat\psi$ as a small classical field, denoted as ψ, with $\exp(-i\mu t/\hbar)(\Phi + \psi)$ solution of the classical version of Eq. (1) of the main text. One then looks for a normal mode of the form

$$\psi(x,t) = u(x,\omega)e^{-i\omega t} + v^*(x,\omega)e^{i\omega t} \tag{S6}$$

For such a normal mode, the linearization of the Gross-Pitaevskii equation leads to the so-called Bogoliubov-de Gennes equation which reads $\mathcal{L}\,\Xi = \hbar\omega\,\Xi$, where $\Xi(x,\omega) = (u(x,\omega)\,,\,v(x,\omega))^T$ and

$$\mathcal{L} = \begin{pmatrix} H & \Phi^2(x) \\ -(\Phi^*(x))^2 & -H \end{pmatrix}, \tag{S7}$$

with $H = \frac{\hbar^2}{2m}\partial_x^2 + U(x) - 2gn(x) - \mu$. Far upstream, the background density being constant, the eigen-modes behave as plane waves of the form

$$\Xi(x,\omega) = \begin{pmatrix} u(x,\omega) \\ v(x,\omega) \end{pmatrix} \underset{x\to-\infty}{\longrightarrow} e^{iqx} \begin{pmatrix} \exp(ik_u x)\,\mathcal{U}_\omega \\ \exp(-ik_u x)\,\mathcal{V}_\omega \end{pmatrix} \tag{S8}$$

where $\mathcal{U}_\omega$ and $\mathcal{V}_\omega$ are complex constants, their explicit expression can be found in Ref. [1], together with the general expression of $u(x,\omega)$ and $v(x,\omega)$. The same type of behavior is observed downstream. The corresponding dispersion relations are of the form

$$(\omega - V_\alpha q)^2 = \omega_{\rm B}^2(q), \tag{S9}$$

where $\alpha = u$ far upstream and $\alpha = d$ downstream and

$$\omega_{\rm B}(q) = c_\alpha q\sqrt{1 + q^2\xi_\alpha^2/4} \tag{S10}$$

is the Bogoliubov dispersion relation. The asymptotic upstream and downstream dispersion relations are represented in Fig. SF1. One sees in this figure that, for each value of ω, there exists three incoming channels, i.e., three plane waves which group velocity is directed towards the horizon. One of these plane waves lies in the upstream region, we denote it as $u|$in, the two others lie in the downstream region: $d1|$in and $d2|$in.

Once the eigen-modes Ξ has been found for all non-zero frequencies, the eigen-basis needs to be completed with the addition of zero modes for which $\omega = 0$. First, it is clear that $\mathcal{L}$ admits a simple zero mode:

$$\mathcal{L}\,\mathrm{P} = 0\,, \quad \text{where} \quad \mathrm{P} = \begin{pmatrix} \Phi(x) \\ -\Phi^*(x) \end{pmatrix}. \tag{S11}$$

The physical interpretation of the existence of this zero mode is the following: it results from the U(1) symmetry breaking of the condensate wave function and it is a collective mode with no restoring force, which is sometimes denoted as a spurious mode [4, 5]. Indeed, if Φ is a stationary solution of the Gross-Pitaevskii equation, for any arbitrary constant θ, $\Phi_\theta(x) = \Phi(x)\,e^{i\theta}$ is also a stationary solution. Φ_θ tends continuously to Φ when $\theta \to 0$, hence $\delta\Phi = \Phi_\theta - \Phi \simeq i\,\theta\,\Phi$ is a solution of the linearized Gross-Pitaevskii equation. This immediately translates into the fact that $(\delta\Phi, \delta\Phi^*)^T = i\,\theta\,\mathrm{P}$ is a zero mode of $\mathcal{L}$.

Another mode of excitation corresponds to addition of particles to the system [6]. By differentiating the Gross-Pitaevskii equation with respect to the number of particles N, we find the mode Q associated to P:

$$\mathrm{Q} = \begin{pmatrix} q(x) \\ -q^*(x) \end{pmatrix}, \quad \text{with} \quad \mathcal{L}\,\mathrm{Q} = -i\,\frac{d\,\mu}{dN}\,\mathrm{P}, \tag{S12}$$

where μ is the chemical potential of the condensate. The two modes Q and P complete the eigen-basis of $\mathcal{L}$, or, more precisely, make it possible to write $\mathcal{L}$ in a Jordan normal form. The field operator $\hat\psi$ which describes the quantum fluctuations can be now expanded over the scattering modes and the zero modes:

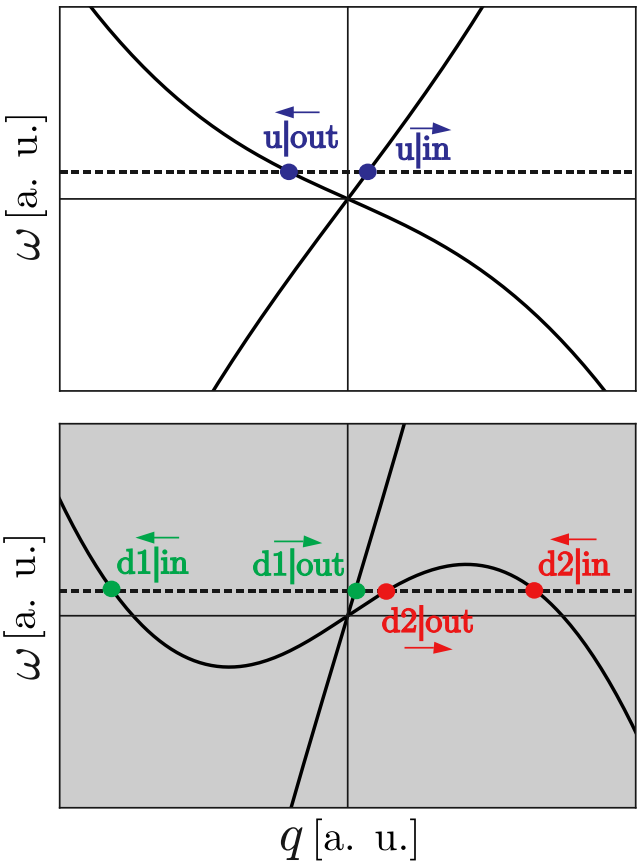

FIG. SF1: Graphical representation of the dispersion relation, i.e., of the solutions of Eq. (S9) in the far upstream (upper plot) and far downstream (lower plot) regions. In the upstream region, for a given ω (represented by a horizontal dashed line) one finds two real solutions of Eq. (S9) which we denote as $q_{u|\rm in}$ and $q_{u|\rm out}$. The intercept of the horizontal dashed line with the corresponding dispersion relation is marked with a colored dot labeled $u|$in or $u|$out, as appropriate. The situation is different downstream: there exists a threshold energy below which Eq. (S9) admits 4 real solutions which we denote as $q_{d1|\rm in}$, $q_{d1|\rm out}$, $q_{d2|\rm in}$ and $q_{d2|\rm out}$. Both $d2$ solutions disappear above the threshold. All these solutions correspond to the channels identified in the main text. They are denoted as "in" ("out") is their group velocity – schematically represented by an arrow – is directed towards (away from) the horizon.

$$\begin{aligned}\hat\psi(x,t) = &- i\Phi(x)\hat{\mathcal{Q}} + iq(x)\hat{\mathcal{P}} + \int_0^\infty \frac{d\omega}{\sqrt{2\pi}} \sum_{L\in\{U,D1\}} \\ &[u_L(x,\omega)e^{-i\omega t}\,\hat b_L(\omega) + v_L^*(x,\omega)e^{i\omega t}\,\hat b_L^\dagger(\omega)] \\ &+ \int_0^\Omega \frac{d\omega}{\sqrt{2\pi}}[u_{D2}(x,\omega)e^{-i\omega t}\,\hat b_{D2}^\dagger(\omega) \\ &+ v_{D2}^*(x,\omega)e^{i\omega t}\,\hat b_{D2}(\omega)].\end{aligned} \tag{S13}$$

In this expression the u_L's and the v_L's are linear combinations of terms of the form (S8) involving the S-matrix (see Refs. [1, 7]), and $\hat{\mathcal{Q}}$ is the phase operator of the condensate, while $\hat{\mathcal{P}}$ corresponds to the fluctuations of the number of particles. The quadratic Hamiltonian $\hat{H}_{\rm quad}$ describing the linear dynamics of the elementary excitations of the system contains a term $\hat{\mathcal{P}}^2/2\,M_{\rm eff}$, where $1/M_{\rm eff} = d\mu/dN$ [4–6]. Thus, the operator $\hat{\mathcal{P}}$ can be identified with a momentum operator and $M_{\rm eff}$ with an effective mass. In addition, the commutation relation $[\hat{\mathcal{Q}}, \hat{H}_{\rm quad}] = i\,\hat{\mathcal{P}}/M_{\rm eff}$ indicates that the phase operator $\hat{\mathcal{Q}}(t)$ is not stationary and deviates from its initial value $\hat{\mathcal{Q}}(t=0)$. This is the phenomenon of phase diffusion, see, e.g, Ref. [8].

In our case, the system is infinite: no phase diffusion can occur and $M_{\rm eff} \to \infty$. The physical interpretation of this phenomenon is that the inertia associated to the change of the global phase of a system of infinite number of particles is infinite. Therefore, the mode Q is also solution of $\mathcal{L}\,\mathrm{Q} = 0$ [see Eq. (S12) with ${}^{d\mu}/_{dN} \to 0$]. Moreover, the operator $\mathcal{L}$ has a different expression for $x<0$ and $x>0$, just because Φ does [see Eq. (S2)]. As a result, $\mathcal{L}$ admits zero energy eigen-states ($\omega = 0$) which have different forms in the upstream and the downstream region. The modes P and Q should be written as linear combinations of these zero modes. In particular, in the upstream region the density profile is a portion of dark soliton [see Eq. (S2)], and the expression of the corresponding zero modes can be found, e.g., in Ref. [9]. One obtains

$$\mathrm{P}(x<0) = \begin{pmatrix} \Phi_u(x) \\ -\Phi_u^*(x) \end{pmatrix} \quad \text{and} \quad \mathrm{P}(x>0) = \begin{pmatrix} \Phi_d(x) \\ -\Phi_d^*(x) \end{pmatrix}, \tag{S14}$$

while

$$\begin{aligned} \mathrm{Q}(x<0) &= i\sqrt{n_u}\,A\left[\cos\theta\tanh(x\cos\theta/\xi_u) - \frac{\Lambda_u}{2}\right]^2 e^{\Lambda_u\,x/\xi_u}\begin{pmatrix} e^{i\,k_u\,x} \\ e^{-i\,k_u\,x}\end{pmatrix} \quad \text{and} \\ \mathrm{Q}(x>0) &= B\begin{pmatrix} \Phi_d(x) \\ -\Phi_d^*(x)\end{pmatrix} + C\,e^{i\,K_0\,x/\xi_d}\begin{pmatrix} [K_0/2 - M_d]\,\Phi_d(x) \\ [K_0/2 + M_d]\,\Phi_d^*(x)\end{pmatrix} + C\,e^{-i\,K_0\,x/\xi_d}\begin{pmatrix} [-K_0/2 - M_d]\,\Phi_d(x) \\ [-K_0/2 + M_d]\,\Phi_d^*(x)\end{pmatrix}, \end{aligned} \tag{S15}$$

with $\Lambda_u = 2\sqrt{1-M_u^2} = 2\cos\theta$ and $K_0 = 2\sqrt{M_d^2-1}$, where M_u and M_d are the upstream and downstream Mach numbers ($M_\alpha = V_\alpha/c_\alpha$). In expression (S15), the normalization factors A, B and C are dimensionless real numbers which are determined by imposing the matching conditions at $x=0$ and the commutation relation between $\hat{\mathcal{Q}}$ and $\hat{\mathcal{P}}$: $[\hat{\mathcal{Q}}, \hat{\mathcal{P}}] = i$, or equivalently, $\mathrm{Q}^\dagger\,\sigma_z\,\mathrm{P} = i$, where σ_z is the third Pauli matrix.

FOURIER TRANSFORM OF THE DENSITY CORRELATION FUNCTION

The computation of the Fourier transform of the G_2 function gives access to the correlation signal between the Hawking pair $[k_{\rm H}(\omega), k_{\rm P}(\omega)]$ in momentum space for a fixed energy $\hbar\omega$ in the lab frame, see Eq. (5) of the main text. The wave vectors $k_{\rm H} = q_{u|\rm out}(\omega)$ and $k_{\rm P} = -q_{d2|\rm out}(\omega)$ are the momenta relative to the condensate of the Hawking quantum and of its partner (see the discussion in Ref. [7]). We define

$$I(\omega) = \frac{1}{\sqrt{n_u\,n_d\,L_u\,L_d}} \times \int_{-L_u}^{0} dx \int_0^{L_d} dx'\, e^{-i(k_{\rm H}(\omega)\,x + k_{\rm P}(\omega)\,x')}\,G_2(x,x'), \tag{S16}$$

where G_2 is the density correlation function [Eq. (4) of the main text]. The quantities n_u and n_d are the asymptotic densities in both regions (when $x \to -\infty$ and $x' \to +\infty$).

As proved in Refs. [7, 10], the integration in Eq. (S16) should be performed over a domain $[-L_u, 0] \times [0, L_d]$ which is adapted to each Hawking pair $[k_{\rm H}(\omega), k_{\rm P}(\omega)]$: one should verify

$$L_u\,V_{g,\rm P}(\omega) = L_d\,|V_{g,\rm H}(\omega)|\ , \tag{S17}$$

where

$$V_{g,\rm I}(\omega) \equiv \left.\frac{\partial\omega}{\partial k}\right|_{k_{\rm I}}, \ \mathrm{I} \in \{\mathrm{H},\,\mathrm{P}\}. \tag{S18}$$

This condition has a physical interpretation: the time taken by an elementary excitation pertaining to the Hawking channel to go from the horizon to the center of the upstream window $[-L_u, 0]$ has to be the same as the time taken by its partner to go from the horizon to the center of the downstream window $[0, L_d]$. The Fourier transform can be calculated theoretically for $L_u,\ L_d \to +\infty$ [still verifying (S17)] and this leads to Eq. (5) of the main text, i.e.:

$$I(\omega) = \mathcal{S}_0\,S_{ud2}(\omega)\,S_{d2d2}^*(\omega). \tag{S19}$$

Fig. SF2 compares the numerical computation of the Fourier transform (S16) (black dots), when the choice of

the window $[-L_u, 0] \times [0, L_d]$ respects condition (S17), with the theoretical expectation [left hand side of Eq. (S19), red curve in the figure]. We observe a nice agreement, except, of course, for long wavelengths where the validity condition of Eq. (S19): $k_{\rm H} L_u$ and $k_{\rm P} L_d \gg 1$ is violated.

The choice of the window is crucial; for example, the orange triangles in Fig. SF2 are obtained for another prescription which corresponds to the long wavelength limit of Eq. (S17):

$$L_u\, V_{g,\rm H}(0) = L_d\, |V_{g,\rm P}(0)|\,, \tag{S20}$$

where $V_{g,\rm H}(0) = V_u - c_u$ and $V_{g,\rm P}(0) = V_d - c_d$ are the group velocities of the Hawking quantum $k_{\rm H}$ and its partner $k_{\rm P}$ in the long wavelength limit. As expected, the result deviates from the evaluation which uses the correct condition (S17).

To recover the numerical result obtained by using the prescription (S20), we use the following approximations: (i) we assume that $k_{\rm H}(\omega) = \omega/(V_u - c_u)$ and $k_{\rm P}(\omega) = \omega/(V_d - c_d)$, as if we were in the dispersionless regime for all frequencies ω, and (ii) we also assume that $S_{ud2}(\omega) \simeq n_{T_{\rm H}}(\omega)$, with $n_{T_{\rm H}}(\omega)$ (the Bose thermal distribution at the Hawking temperature) and that $|S_{ud2}|^2\, |S^*_{d2d2}|^2 \simeq n_{T_{\rm H}}(\omega)(1 + n_{T_{\rm H}}(\omega))$ [Eq. (8) of the main text]. Then, we compute expression (S19) using both approximations (i) and (ii): we obtain the dark blue curve in Fig. SF2 which agrees well with the orange triangles.

In conclusion, one may numerically analyse the information contained in the density distribution G_2 by using Eq. (S16) within the oversimplified long wavelength prescription (S20) and still get an equality between the two terms of Eq. (S19). However, this approach could lead to the erroneous conclusion that the analogous Hawking radiation is thermal for all frequencies ω. In our system, where dispersion plays an important role, only the result represented by the red curve in Fig. SF2 should be considered as correct, and it clearly deviates from the thermal result (dark blue curve in Fig. SF2).

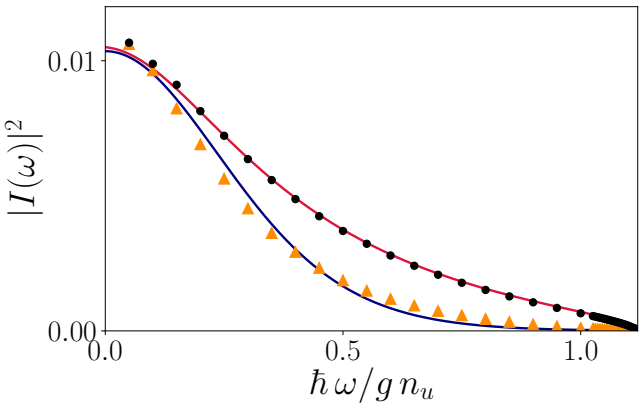

FIG. SF2: Fourier transform of the G_2 function, denoted as $I(\omega)$ and given by expression (S16), plotted as a function of ω. The red curve indicates the theoretical expectation: right hand side of Eq. (S19). The black dots are obtained by the numerical computation of the Fourier transform (S16) with condition (S17). The orange triangles are also obtained numerically, but for a different choice of window corresponding to prescription (S20). The dark blue curve is obtained from (S19) but in the long wavelength approximation, where the analogous Hawking signal is thermal.

EFFECT OF TEMPERATURE ON THE DENSITY CORRELATION FUNCTION

In this section, we discuss how to account for temperature effects in our system. We first note that the stationary configuration we consider is thermodynamically unstable, and cannot support a thermal state. However, a thermal-like occupation of the states can be defined as detailed for instance in Ref. [7]. Previous studies [11] have already highlighted the robustness of the correlation signal, even if the temperature of the system is greater than the Hawking temperature. Our results confirm this point, as shown in Fig. 3 of the main text (the orange solid line is the finite temperature result for $k_B\, T = 0.2\, g n_u \simeq 1.9\, T_{\rm H}$). At finite temperature, the density correlation function $G_2(x, x')$ splits in two parts [1, 11]:

$$G_2(x, x') = G_2^0(x, x') + G_2^T(x, x'), \tag{S21}$$

where G_2^0 is the zero temperature contribution and G_2^T accounts for the additional temperature effects. As already mentioned in Refs. [11, 12], G_2^T contains a term which corresponds to a thermal enhancement of zero temperature correlations, together with additional contributions involving scattering processes specific to the $T \neq 0$ case. This results in a practical disappearance of the $u|\text{out} - d1|\text{out}$ correlation for $k_B\, T \simeq 0.2\, g n_u$, while the $u|\text{out} - d2|\text{out}$ Hawking signal is robust up to $k_B\, T \simeq g n_u$, see the discussion in Ref. [11]. This confirms the interest of using analog system to investigate analog Hawking radiation: the non-local correlation pattern in G_2 is weakly affected by temperature and a noticeable signal can be recorded even if T is larger than $T_{\rm H}$.

The finite T result presented in the main text is obtained by computing the two contributions in (S21) separately, in a regime which has been denoted as the "weakly interacting quasicondensate regime" in Ref. [13], and which holds when the following conditions are met:

$$\frac{4\,\tau_\alpha^2}{(\xi_\alpha\, n_\alpha)^4} \ll \frac{1}{(\xi_\alpha\, n_\alpha)^2} \ll 1, \tag{S22}$$

where $\alpha \in \{u, d\}$ and $\tau_\alpha = k_B\, T/(g\, n_\alpha)$ is the reduced temperature. We use typical experimental parameters of Ref. [3] to evaluate the order of magnitude of the

different terms in the inequalities (S22): $\xi_u = 1.4\,\mu$m, $\xi_d = 2.38\,\mu$m, $n_u \simeq 70-90\,\mu\text{m}^{-1}$ and $n_d \simeq 20\,\mu\text{m}^{-1}$. We obtain $(\xi_u\, n_u)^{-2} \simeq 6.3\times10^{-5} - 10^{-4} \ll 1$, $(\xi_d\, n_d)^{-2} \simeq 4.4\times10^{-4} \ll 1$. By computing the left hand part of (S22) in the upstream and downstream regions, we find that the more stringent condition reads $k_B\, T \ll 8.3\, g n_u$, i.e., our approach is valid up to $k_B\, T \simeq 0.8-1\, g n_u \gg T_{\text{H}}$.

[1] P.-É. Larré, A. Recati, I. Carusotto, and N. Pavloff, Phys. Rev. A **85**, 013621 (2012).

[2] P. Leboeuf, N. Pavloff and S. Sinha, Phys. Rev. A **68**, 063608 (2003).

[3] J. R. M. de Nova, K. Golubkov, V. I. Kolobov, and J. Steinhauer, Nature (London) **569**, 688 (2019).

[4] P. Ring and P. Shuck, *The Nuclear Many-Body Problem* (Springer-Verlag, Berlin, 1980).

[5] J. P. Blaizot and G. Ripka, *Quantum Theory of Finite Systems* (MIT Press, Cambridge, MA, 1986).

[6] C. J. Pethick and H. Smith, *Bose-Einstein Condensation in Dilute Gases*, (Cambridge University Press, Cambridge, England, 2002).

[7] A. Fabbri and N. Pavloff, SciPost Phys. **4**, 019 (2018).

[8] P. Villain, M. Lewenstein, R. Dum, Y. Castin, L. You, A. Imamoğlu, and T. A. B. Kennedy, J. Mod. Optics **44**, 1775 (1997).

[9] N. Bilas and N. Pavloff Phys. Rev. A **72**, 033618 (2005).

[10] J. R. M. de Nova, F. Sols and I. Zapata, New. J. Phys. **17**, 105003 (2015).

[11] A. Recati, N. Pavloff and I. Carusotto, Phys. Rev. A **80**, 043603 (2009).

[12] J. Macher and R. Parentani, Phys. Rev. A **80**, 043601 (2009).

[13] P. Deuar, A. G. Sykes, D. M. Gangardt, M. J. Davis, P. D. Drummond and K. V. Kheruntsyan, Phys. Rev. A **79**, 043619 (2009).